Multiple Type Grid Approach for 3D Process Simulation

D. Kimpton, M. Baida, V. Zhuk, M. Temkin and I. Chakarov
Silvaco International, 4701 Patrick Henry Drive, Bldg. 2
Santa Clara, CA 95054, U.S.A.
E-mail: ivan.chakarov@silvaco.com

***Abstract*—Various aspects of discretization and data representation in a generic 3D process simulator are discussed. It is shown that the only practical way to provide the efficient and robust simulation of various process steps is to use application specific gridding and numeric methods for distinct process step and provide smooth synchronization and data transformation between the simulation modules. We demonstrate how this approach can be successfully used for simulation of complete 50 nm MOSFET device cell starting from the physical layout and finish with simulation of its IV characteristics using the device simulator ATLAS3D.**

Etching; deposition; annealing; implantation; process; device; simulation; ATLAS3D;

I. INTRODUCTION

Ongoing transition from 2D to 3D process simulation requires careful consideration of numerical methods and corresponding spatial discretisation techniques most suitable for efficient computation of each technological step and a complete process flow. In traditional approach, one type of grid is used throughout all simulation steps. In case of 2D simulation, various triangle grids with some local re-gridding prove to be sufficient though not always convenient and efficient. However, the direct propagation of this approach into 3D with exclusive use of thetrahedral grids appears to encounter many difficulties. In this paper we demonstrate more flexible approach in which different types of grids are used for different simulation steps inside a 3D process simulator.

The implemented data model is based on the fact that tetrahedral meshes can effectively and exactly represent material regions and interfaces, whereas irregular Cartesian (rectilinear) grids are mostly suitable for volumetric physical data representation. A Delaunay tetrahedral mesh serves as a geometrical skeleton optimally coarsened to reduce computer memory requirements. The main advantages of this approach are speed and the ability to handle structures featuring large aspect ratios. The tetrahedra based geometrical grid also has following purposes, *a)* it serves as an initial and final state for etching and deposition, *b)* it defines the geometrical topology needed in ion implantation and *c)* it acts as a geometrical server, i.e. keeping and issuing all kind of information related to regions, materials and interfaces. Physical data such as doping concentrations, damage etc., are all kept on the irregular Cartesian grid. Two types of nodes are used to store the data, the 'regular' nodes, according to rectilinear grid and the 'boundary' nodes representing values at the intersection of the Cartesian grid and the material interfaces. Three dimensional interpolation techniques are used during synchronization of the two grids to correctly represent physical values after change of geometry, i.e. move of boundaries. The created immersed boundaries rectilinear grid is further used for simulation of implantation, annealing steps and device simulation as well.

II. A GENERIC METHOD FOR TRACKING FRONTS IN ETCHING AND DEPOSITION

Any semiconductor device manufacturing flow includes many process steps, which change geometry of the device structure. Material etching and deposition are main technological methods used to build desirable device structures. Efficient and robust modeling of multiple deposition and etching steps is an important part of any 3D process simulation system. The key numerical and gridding problem for etch and deposition simulation is accurate tracking of the moving boundary front. The methods for solving moving boundary problems could be roughly divided into four distinct groups: string-based, cell-based, level-set and volume-of-fluid methods. Each of these methods have their advantages and serious difficulties depending mainly on the size and discretization of simulation domain and complexity of physical models for etching and deposition.

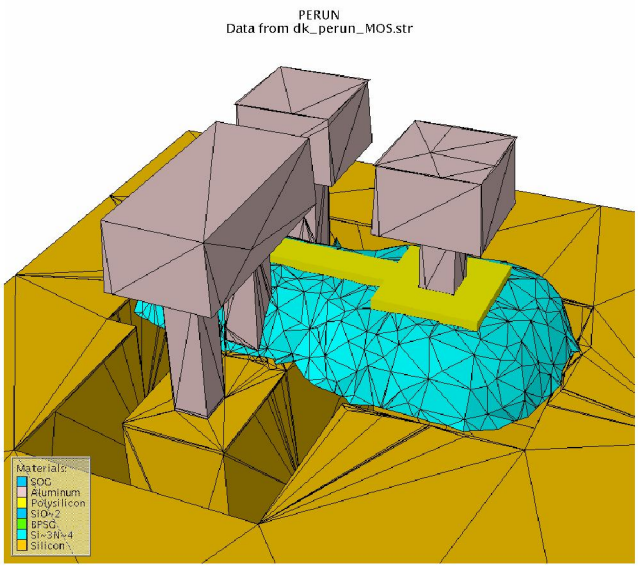

Figure 1. A 50nm MOSFET cell showing trench isolation, spacer, polisilicon gate, and four electrodes.

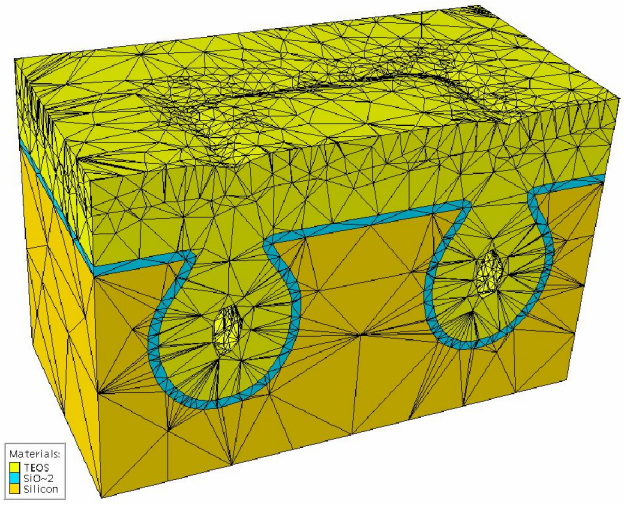

Figure 2. Final trench refill demonstrating void creation.

We have found that the 3D extension of a string algorithm based on the adaptive refinement of a tetrahedral grid [1,2] is the most suitable approach for simulation of etching and deposition steps of the typical process flows discussed in this paper. In most cases, it is sufficient enough to consider conformal or "step coverage" deposition and arbitrary combination of directional and isotropic etching. The algorithm described in [1] tracks the boundary front after each time step in case of "physical" etching and deposition or captures the final boundary position in case of "geometrical" (or user-defined) removal or addition of a material layer.

The moving front calculated from etching or deposition rates or specified geometrically by user is *implicitly* represented in a tetrahedral mesh. Adaptive mesh refinement with a user defined resolutions is applied to only those tetrahedra, which are intersected by the front. After that the new front is extracted by splitting and classifying new tetrahedra. This approach is as efficient as the string algorithm in 2D and as robust as level-set method in solving difficult problems of de-looping and void formation.

Fig. 1 and 2 represent an illustration of the tetrahedral grid generated for a complex 3D process with several etching and deposition steps.

III. Immersed Boundary Rectilinear Grids and 3D Diffusion Simulation

In order to calculate dopant redistribution and activation during the anneal process step, the finite difference method is elaborated for numerical solution of systems of partial differential equations in complex geometries.

The representation of the simulation domain is based on an immersed boundary grid model, in which the interfaces of a complex region are cut across an irregular rectilinear Cartesian grid. As a result, it is possible to use easy accessible data storage for structured nodes and an additional set of data for interface nodes along each grid line. This allows to employ the highly efficient and well understood methods in the regions away from the boundary, and confines the use of specific integration approach near the interfaces.

As a basic diffusion model in silicon, the Fermi model is chosen with possibility of future enhancement. The numerical implementation is based on extension in 3D of approaches from [3]. The set of diffusion equations is discretized by using the splitting technique and conservative integration scheme along the linear intervals within homogeneous material. The backwards Euler scheme is used for time integration. Gauss-Seidel iterative method is exploited to solve the non-linear equations that arise at each time step. The linear solver is based on Gauss elimination that takes into account the specific sparse matrix structure.

The developed algorithms are realized for 3D geometries with static piece-wise smooth boundaries. The irregular rectilinear mesh is kept fixed during the calculations. There is an option to make 'rough' but fast preliminary calculation followed by the simulations on the mesh optimized in areas of interest to provide needed accuracy. Such an approach overcomes most of the 3D process simulation difficulties, i.e. huge computer memory requirements, low computational efficiency and convergence problems associated with poor unstructured grid quality.

IV. Physically Based Model for 3D Ion Implantation

A general purpose *Monte Carlo* (MC) simulator for particle transport in arbitrary 1, 2 and 3D topologies has been implemented. It's main purpose is the simulation of ion implantation using physically-based models for stopping and ranges. It is capable of simulating implants into arbitrary surface topography and implant window sizes.

The standard approach to the 2D and 3D ion implantation simulation has been to make use of analytical 1D profiles tabulated over wide energy range and ion doses. These are then given a lateral Gaussian tail in order to simulate the 3D dopant density distribution. The parameters for the 1D profiles are obtained either by simulation or experiment. The analytical model is well suited for deep well implants.

The above approach is approximate, neglecting the detailed effects of transport through varying topography and materials, as well as damage build-up in the crystalline regions. Using the older MC model from the 2D process simulator for implants into large 3D structures has not been practical due to the very long computation times involved. Our newly developed MC implantation simulator uses numerous algorithms to enhance the computational efficiency of ion implant simulation, thus being able to perform simulations into large structures in a reasonable amount of time, eliminating or reducing the need for approximate 3D analytical models. The MC implantation simulator could be divided into three logically separate units – physical model, topography and target description and optimization/acceleration algorithms.

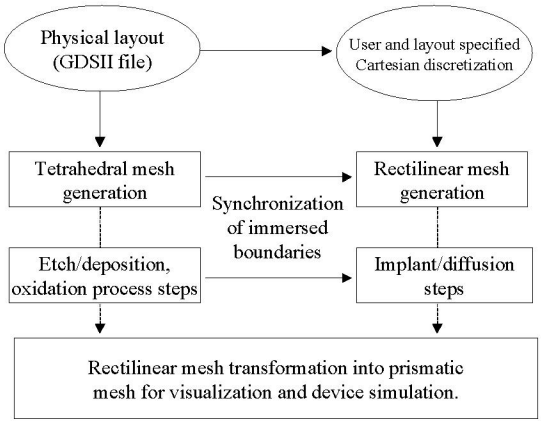

Figure 3. Block diagram of multiple grid process flow.

Advanced physical model is critical for a predictive ion implantation and our implementation in the MC simulator is described elsewhere, [4,5]. To keep the efficiency of the algorithm, the damage model implemented is that of Kinchin-Pease, [6,7]. The interstitial and vacancy concentrations are derived from the Frenkel pairs (FP) distribution, differing only by the impurity concentration (the so called "+1" model). It is possible to modify this behavior to "+n", which is more suitable for heavy ions. The simulator maintains its own adaptive grid, which fits to the desired topology, thus, treating effectively shadowing, reflection and re-implantation effects. One of the critical and time consuming tasks of MC ion implantation in crystalline materials is finding the neighboring atoms for interaction. Because of crystal symmetry, a special search algorithm needs to be implemented. The present algorithm implements special look-ahead techniques, which, compared to previous 2D MC simulator, accelerate three to four times the finding of a collision partner. In addition, a *rare-event* and a *stratified-sampling* algorithms are implemented in order to improve statistics along depth or about fine special details in the topology. Furthermore, in case of simple topologies, the program can use trajectory replication for flat, i.e. 1D in character, regions. A more sophisticated trajectory replication algorithm, based on pattern recognition and classification, is under development, which promises to optimally reduce computational time for arbitrary in complexity structures.

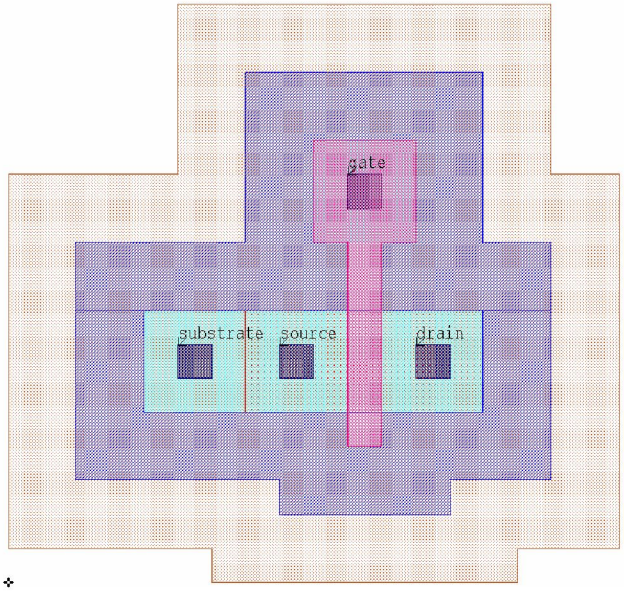

Figure 5. Physical layout of the MOSFET cell used in complete process flow. The simulator reads a GDSII format file, which can be created with a layout editor.

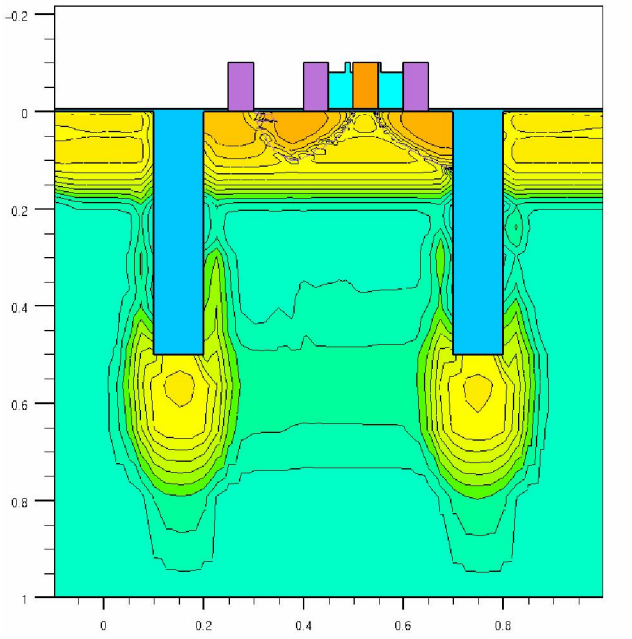

Figure 4. Cross section along source – drain electrodes of the MOSFET cell, showing the net doping after annealing.

V. Example of Complete Process Flow

Our process simulator is designed to support the complete process flow starting from mask layout and proceeding through all structure transformation steps even some of these steps are simulated using simplified models (e.g. dry or vertical etch). This approach provides users with better practical capabilities to analyze layout, process and geometrical feature variations than simulators based on mechanical CAD style "device builders".

The complete process simulation flow is shown in Fig. 3. The GDSII layout file is loaded into the process simulator which selects the masks and performs corresponding structure transformation process steps (etching, deposition, etc.) by generating optimal tetrahedral mesh after each such step. Simultaneously, the Cartesian rectilinear mesh is generated out of user and layout specified discretisation and immediately starts synchronizing it's immersed boundaries with the geometrical (i.e. tetrahedral mesh). The frequency of synchronization depends on how often the implant or diffusion statements are used, and, it is triggered when tetrahedral mesh has changed, which is usually after each etch and deposition or mask photoresist statements. After each synchronization, the rectilinear mesh does appropriate interpolation between the

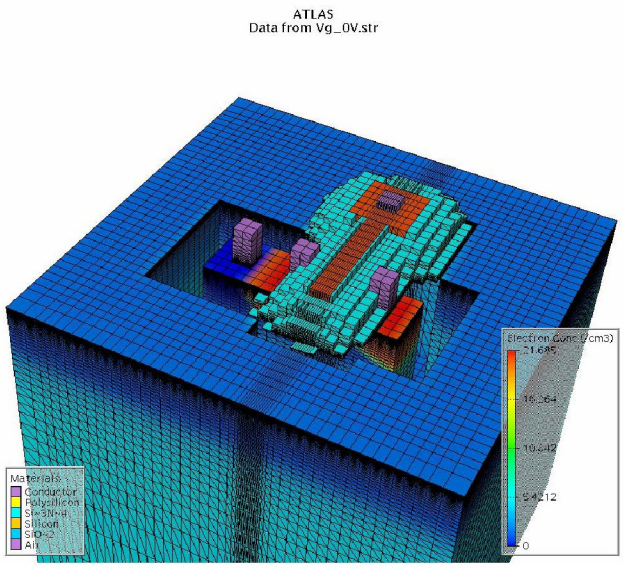

Figure 6. The MOSFET cell showing electron density distribution transformed into a prismatic grid structure used by the device simulator.

'old' and 'new' immersed boundaries, thus, keeping all physical data intact.

Figs. 4 through 7 present different elements of process and device simulation of complete 50nm MOSFET using the above described simulation flow. Fig. 5 depicts the physical layout used to build the device. Through mask statements from the layout, the process simulator deposits photoresist, and then uses etch/deposit and oxidation statements to progressively build the device in a manner highly reflective of the realistic fabrication process. For final importation into a 3D device simulator, the structure grid is converted into the optimal format for the chosen simulator, in this example being ATLAS3D, Fig.6. Experience has shown us that the prismatic grid is optimal for mathematical convergence when solving the Jacobian matrix associated with device physics equations. Converging the grid in this way allows the use of already available mature device simulators permitting all manner of other stimuli to be simulated such as optical interactions, self heating, and transient effects for to name a few.

VI. Conclusion

A practical, memory efficient, and very fast 3D process simulator has been demonstrated by using an approach, which

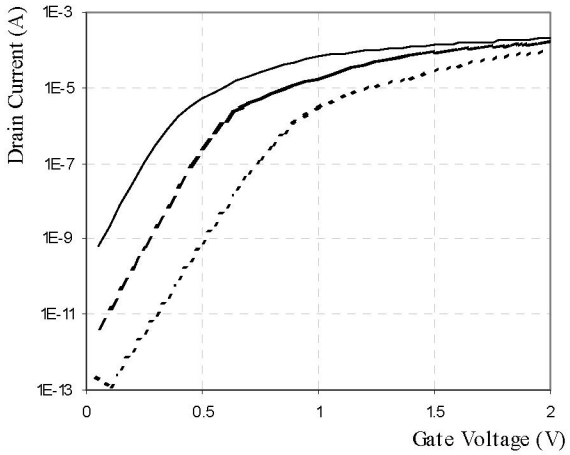

Figure 7. Sub-threshold IV characteristics for different "Vt" implant doses.

utilizes the most efficient gridding system for each of the process and device simulation steps. By using this "multiple gridding" approach, many of the compromises of using only one type of gridding method for the whole simulation are thus eliminated, reducing simulation times for 3D TCAD down to very reasonable and practical levels.

References

[1] A. Liu amd M. Horlacher, Proceedings of 8th international meshing roundtable, pp. 333–343, 1999.

[2] A. Liu and M. Baida, Proceedings of 9th international meshing roundtable, pp. 307–315, 2000.

[3] V. A. Zhuk, Engineering Simulation, vol. 14, p. 959, 1997.

[4] I. Chakarov and R. Webb, Radiat. Effects Defects Solids, vols. 130–131, pp. 445–447, 1994.

[5] I. Chakarov and M. Temkin, "Modelling of ion implantation in SiC crystals," Nucl. Instr. Methods Phys. Res., vol. B242, pp. 690–692, 2006.

[6] G. H. Kinchin and R. S. Pease, "The displacement of atoms in solids by radiation," Rep. Progress Phys., vol. 18, pp. 1–51, 1955.

[7] M. J. Norgett, M. T. Robinson, and I. M. Torrens, "A proposed method of calculating displacement dose rates," Nucl. Eng. Des., vol. 33, pp. 50–54, 1975.